

論文 / 著書情報
Article / Book Information

Title	Shaking table tests on the lateral response of a pile buried in liquefied sand
Authors	Jonathan R. Dungca, Jiro Kuwano, Akihiro Takahashi, Takashi Saruwatari, Jun Izawa, Hiroko Suzuki, Kohji Tokimatsu
Citation	Soil Dynamics and Earthquake Engineering, Vol. 26, pp. 287-295
Pub. date	2006, 2
DOI	http://dx.doi.org/10.1016/j.soildyn.2005.02.021
Creative Commons	See next page.
Note	This file is author (final) version.

License



Creative Commons: CC BY-NC-ND

Shaking table tests on the lateral response of a pile buried in liquefied sand

J.R. Dungca¹, J. Kuwano¹, A. Takahashi², T. Saruwatari¹, J. Izawa¹, H. Suzuki³, K. Tokimatsu³

1 Department of Civil Engineering, Tokyo Institute of Technology, Japan

2 Public Works and Research Institute, Japan

3 Department of Architecture and Building Engineering, Tokyo Institute of Technology, Japan

Abstract

This paper presents an experimental study on the lateral resistance of a pile subjected to liquefaction-induced lateral load. To observe the soil surrounding the pile during liquefaction, it was modeled as a buried cylinder that corresponded to a sectional model of the prototype pile at a certain depth in the subsoil. In order to create a realistic stress condition in the model ground, the model was prepared in a sealed container and the overburden pressure was applied to the ground surface by a rubber pressure bag. The model pile was actuated back and forth through rods attached on each side by an electro-hydraulic actuator.

This paper focuses on observing the deformation of the liquefied soil surrounding the pile when a large relative displacement between the pile and the soil is induced. The loading rate effect on the lateral resistance of the pile in the liquefied sand and the influence of the relative density are also investigated.

Test results show that a larger resistance is mobilized as the loading rate becomes higher. When the loading rate is higher, the cylinder displacement required for the lateral resistance becomes smaller. It has been also observed that as the relative density of the soil increases, dilatancy of the soil in front of the pile also increases.

Key words: Liquefaction; Pile; Shaking table test

Soil Dynamics and Earthquake Engineering, 26, 287-295, 2006

Official URL:

<http://dx.doi.org/10.1016/j.soildyn.2005.02.021>

1 **1. Introduction**

2 One of the major sources of earthquake-induced damage to port facilities is liquefaction of
3 saturated loose sandy soils. This type of soil failure often prevails at waterfronts and marine
4 environments. The significant liquefaction and associated ground movement and waterfront
5 structure damage have not only occurred under very strong earth-quakes like the 1995 Hyogo-ken
6 Nambu Earthquake (Kobe earthquake), but also under moderate levels of earthquake motion in
7 past earthquakes (Technical Council on Lifeline Earthquake Engineering of ASCE [14]). For
8 instance, port facilities experienced severe damage due to liquefaction at the Port of Oakland and
9 the Port of San Francisco during the 1989 Loma Prieta Earthquake in USA, although recorded
10 peak horizontal accelerations at those locations were 0.29 and 0.15 g, respectively.

11
12 Near waterfronts many pile-supported structures, especially pile-supported buildings, had pile
13 damages without severe damage to their superstructures. During the lateral spreading of liquefied
14 soil, the covering non-liquefied soil, i.e. the soil layer above the water table, moves seaward
15 together with the liquefied soil. Pile foundations located in such a lateral spreading ground were
16 investigated by various researchers(Abdoun and Dobry [1], Horikoshi et al. [5] and Takahashi et
17 al. [11], detailed observations revealed that damages to the pile occurred at depths other than the
18 pile heads, particularly near the interface between liquefied and non-liquefied soils. Development
19 of large strains in liquefied soil layer can induce high bending moments in piles that extend
20 through it. Hence, around an interface between liquefied and non-liquefied soil, a significant
21 curvature will be demanded on a pile due to the difference in soil stiffness. In other words, the
22 lateral resistance of the pile drastically changes along the pile length.

23
24 In non-liquefied soils, the lateral resistance of a pile maybe evaluated by solid mechanics based
25 on concepts of effective stress, though several difficulties arise for partially saturated soils above
26 the groundwater. On the other hand, pile resistance in the liquefying soil drastically changes with
27 the accumulation of excess pore water pressure during an earthquake. Some researchers have put
28 forward a hypothesis that the liquefied soil behaves as a liquid. For instance, Hamada et al. [3]
29 and Satoh et al. [10] conducted shaking table tests in 1 and 50 g, respectively, on the dynamic
30 behavior of a single pile in sloping liquefied sand. They showed that the bending strain of the pile
31 first increased and then dropped to almost zero during the shaking.

32
33 This fact supports the hypothesis that the liquefied soil behaves as a liquid, and the loading rate
34 affects the lateral resistance of the pile in the liquefied soil. Supposing that the liquefied soil is a
35 kind of incompressible fluid, determination of the viscosity of the fluid is necessary to estimate
36 the lateral resistance of the pile in the liquefied soil, as an object's drag force in the
37 incompressible fluid is characterized by the viscosity when the size of the object and the velocity
38 of the fluid are given. In order to determine the viscosity of the liquefying soil, many
39 experimental researches were conducted in the 1990s (e.g. Miyajima and Kitaura [8] Towhata et
40 al. [15]). However, this idea that the behavior of the liquefied soil can be illustrated by that of an

1 incompressible fluid is not seen to be suitable for the recent performance-based design of pile
2 foundations, as it is very difficult to determine the velocity of the ground shaking during the
3 whole period of the shaking. Without information on the variation of the ground velocity,
4 permanent deformation of the pile foundation cannot be predicted.

5
6 In practical seismic design codes for the piled structures, it is prescribed that the displacements of
7 the pile foundation during earthquakes must be assessed by a framed structure analysis subjected
8 to soil movement through soil-structure interaction springs (Railway Technical Research Institute
9 [9]; Metropolitan Expressway Public Corporation [7]; The High Pressure Gas Safety Institute of
10 Japan [4]. These earthquake resistant design codes in Japan have been summarized by the Japan
11 Society of Civil Engineers [6]. In these codes, a degradation parameter of the lateral resistance in
12 liquefiable soils, which is a reduction parameter of the lateral resistance of the pile in the
13 liquefied soil in relation to that in the non-liquefied soil, is in the range of 1/1000 and 1/100.
14 These reduction factors have been determined by back analyses to fit responses of piles damaged
15 in earthquakes without consideration of the behavior of the soil surrounding the pile. These
16 determinations maybe based on an assumption that the degradation parameter of the lateral
17 resistance of the pile is proportional to an effective confining stress of the subsoil, and the
18 volume of the soil resisting the pile movement is quite limited adjacent to the pile. Dobry et al.
19 [2] showed relationships between the degradation parameter for p-y curves, c_u , and the excess
20 pore water pressure, r_u , obtained from centrifuge model tests. They concluded that the value of
21 lateral forces decreased as the pore pressure ratio increased. However, in the liquefying soil, the
22 behavior of the soil surrounding the pile is still unknown and the lateral resistance mobilization
23 mechanism is also not clarified. Hence, direct measurement of the lateral pile resistance in the
24 liquefied soil and observation of the soil surrounding the pile are attempted in this study.

25
26 Information derived from the studies mentioned above is seen to be of value in demonstrating the
27 actual behavior of piles and soils during earthquakes. However, the actual behavior of pile is
28 complicated and affected by several factors. Investigating effects of each factor from the
29 complicated behavior observed in the shaking table tests is not a straight forward process. To
30 easily observe the soil surrounding the pile, it was modeled as a buried cylinder that represents a
31 sectional model of a pile at a certain depth in the subsoil (Fig. 1). Measurements of the drag force
32 of the cylinder embedded in sand were based on the experiment done by Towhata et al. [15]. In
33 order to create a realistic stress condition in the model ground, the model was prepared in a
34 sealed container and the overburden pressure was applied to the ground surface by a rubber
35 pressure bag.

36
37 This study focuses on observing the deformation of the liquefied soil surrounding the pile when a
38 large relative displacement between the pile and the soil is induced. The loading rate effect on the
39 lateral resistance of the pile in the liquefied sand and the influence of the relative density are also
40 investigated (Takahashi et al. [12]).

1 2. Methodology

2 2.1. Test procedures

3 The model setup used in this study is schematically illustrated in Fig. 2. An aluminum model
4 container was used with inner sizes of 450 mm in width, 150 mm in breadth, and 250 mm in
5 height. To observe the deformation of the model ground during the test, the front face of the box
6 was made transparent. A rubber pressure bag was attached underneath the top lid of the container
7 to apply an overburden pressure, P_o , on the surface of the soil. A fluid tank was connected at the
8 bottom of the box to supply and drain out fluid and to apply a back pressure, P_B , to the pore fluid
9 of the soil. The picture of the actual experimental setup is shown in Fig. 3.

10
11 Fig. 4 shows an aluminum-made-cylinder equipped with pore and earth pressure transducers. The
12 surface of the cylinder was fabricated smoothly. Rubber sheets were put on both ends of the
13 cylinder for lubrication and to prevent sand particles from getting into the gap between the
14 cylinder and the side walls of the container. Two rods were connected to the center of the
15 cylinder. Two load cells were inserted into the respective rods near the cylinder to avoid the
16 influence of friction in measuring the net lateral force on the cylinder. The cylinder was actuated
17 back and forth through the rods by an electro-hydraulic actuator. The actuator was mounted on
18 the side wall of the model container.

19
20 Toyoura sand, uniformly graded sub-angular quartz sand ($D_{50} = 0.19$ mm), was used for the
21 model. The model ground was prepared by the air pluviation method to achieve different relative
22 densities desired. Different test conditions with different relative densities were prepared in this
23 study to evaluate the effect of the liquefied ground surrounding the pile during an earthquake.
24 The model ground was saturated up to the ground surface with de-aired water or methyl cellulose
25 solution under a negative pressure of 98 kPa in a large tank by applying a vacuum. Japanese
26 noodles, 'somen', were placed between the model ground and the transparent window as markers
27 to observe the deformation of the ground. After the saturation, the top lid of the box was attached
28 and the over burden pressure was applied to the soil under the drained condition.

29
30 After preparing the model ground, the container was set on the mechanical shaker (Takemura et
31 al. [13]) and the electro-hydraulic actuator was attached to it. During tests, the horizontal shaking
32 of the container started two seconds prior to the pile loading. This duration was enough to liquefy
33 the model ground. A horizontal shaking was applied to the container by sinusoidal waves with a
34 frequency of 50 Hz and a maximum acceleration of approximately 5 g. The period of shaking
35 was 10 s. During the tests, acceleration of the container, horizontal load and displacement of the
36 cylinder, and earth pressure and pore fluid pressure around the cylinder were measured.
37 Movement of the cylinder and the ground was recorded by a digital video camera (Takahashi et
38 al. [12]).

39

1 2.2. Test conditions

2 Two sets of test conditions were prepared in this study. The first test condition is shown in Table
3 1. In this test condition, the effect of ground vibration and loading rate of the cylinder on the
4 lateral resistance of the cylinder were investigated. In all the cases, the applied over burden
5 pressure was $P_o = 49$ kPa. The loading rate of the cylinder, V , was varied from 1 to 100 mm/s. In
6 the cyclic loading tests, the symmetrical triangular waves were applied in order to achieve a
7 constant loading rate. The relative density used in this test condition is 40%.

8
9 In cases SW1, SW10, SW100, SM1, SM10 and SM100, a horizontal sinusoidal motion was
10 applied to the container to generate the excess pore fluid pressure in the model. Meanwhile, in
11 cases SW1Q and SW10Q, pore pressure increase, P_B , of 49 kPa was applied to the soil after the
12 consolidation of the soil at $P_o = 49$ kPa without ground vibration. The effective confining stress
13 of the model became almost zero by increasing the back pressure without ground vibration on the
14 condition that the model was subjected to almost the same stress history that the models in the
15 other cases experienced. This stress condition is defined as artificial soil ‘liquefaction without
16 ground vibration’ in this study. SM10N and SM100N were the tests in which the cylinder was
17 moved back and forth with the initial condition of no liquefaction.

18
19 At the beginning, de-aired water was used as the pore fluid. However, considering the partial
20 drainage around the cylinder, the migration velocity of water was relatively large, as the diameter
21 of the cylinder was very small compared with the actual pile. In order to consider this problem, in
22 the latter half of the series of the tests, the scaling laws of the centrifuge modeling were adopted,
23 i.e., a higher viscosity fluid (methyl cellulose solution) was used as the pore fluid to avoid
24 conflict with the scaling laws for the time of dynamic events and seepage. The viscosity of the
25 methyl cellulose solution was 50 times higher than that of fresh water. With this similitude rule,
26 measured lateral resistance of the 20 mm-diameter cylinder corresponds to the lateral resistance
27 of the 1 m-diameter pile at a depth of 5 m. Loading rate of 1 mm/s corresponds to the situation of
28 the pile in a very slow flow of liquefied soil, while that of 100 mm/s corresponds to the vibration
29 of the pile during an earthquake (Takahashi et al. [12]).

30
31 Table 2 shows the second test condition. In this test condition, different relative densities of the
32 ground were prepared to evaluate its effect on the pile. In the column under ‘Case’, ‘L’ means the
33 ground is in the loose condition, ‘M’ means the ground is in the medium dense condition and ‘D’
34 means the ground is in its dense condition. The next number next to these letters, 1, 10 and 100,
35 refer to loading rates of the cylinder (For example, L10 means the density of the ground is in the
36 loose condition and the loading rate of the cylinder is 10 mm/s). Only methyl cellulose solution
37 was used to saturate the ground for all the cases in this test condition. All other parameters are the
38 same as in the first test condition.

39

1 **3. Results and discussions**

2 **3.1. Deformation of the surrounding soil**

3 The deformation of the soil surrounding the pile and the lateral resistance of the pile were
4 evaluated by comparing the effect of the cases with and without container shaking.

5
6 Fig. 5 shows the graph of four cases, SW1Q, SW10Q, SW1, and SW10. No shaking was
7 introduced on the first two cases while shaking was done on the last two cases. The graph is a
8 plot of the normalized lateral resistance of the cylinder, p/p_o against the normalized displacement,
9 called reference strain, $\gamma = \delta/D$. The lateral resistance of the cylinder has been normalized by
10 dividing its value by the initial overburden pressure, $p_o = 49$ kPa. On the other hand,
11 displacement has been normalized by dividing its value by the diameter, D .

12
13 It can be seen from the graphs in Fig. 5 that irrespective of the method of inducing liquefaction,
14 the larger loading rate makes the lateral resistance larger. Regarding the difference in the method
15 used to induce liquefaction, the lateral resistances for cases without ground vibration are
16 remarkably larger than those with vibration.

17
18 Fig. 6 shows the deformation of the soil surrounding the cylinder just after loading. The black
19 lines are the noodle markers placed vertically on the soil before the test. In the cases without
20 ground vibration, it has been observed that a large amount of soil has moved forward resulting to
21 the upheaval of the ground surface. On the other hand, when shaking was applied to the container,
22 the deformation of the soil was quite limited to the areas very close to the cylinder. The
23 difference in the soil area influenced may have directly affected the lateral resistance of the
24 cylinder for the cases of with and without shaking as shown in Fig. 5. The vibration of the ground
25 may have caused instability in the soil particles contact and thus, reduced the resistance of the
26 surrounding soil against the movement of the cylinder (Takahashi et al. [12]).

27 28 **3.2. Loading rate effects on the lateral resistance**

29 The first loops of the relationship between lateral resistance and displacement of the cylinder for
30 cases SM1, SM10 and SM100 for loading rates of 1, 10 and 100 mm/s, respectively, were plotted
31 in Fig. 7. The initial resistance was negligibly small in all the cases. Larger lateral resistance
32 mobilization is evident as the loading rate becomes higher. The lateral resistance was mobilized
33 only after reaching a certain amount of displacement depending on the loading rate.

34

1 The resistance transformation point is defined, in this study, as the point where the gradient of the
2 loop starts to increase. The normalized displacement at the point is referred to as the reference
3 strain of resistance transformation point, γ_L , as shown in Fig. 8. The reference strain is the point
4 that the shear strength of the soil starts to recover in a post-liquefaction stress-strain relationship
5 (Yasuda et al. [16]). Reference strains of resistance transformation points in the first loading
6 against its loading rates were plotted as shown in Fig. 9. In the case of smallest loading rate, as no
7 obvious mobilization of the lateral resistance was observed in the range of the pile displacement,
8 the reference strain must be larger than value shown in Fig. 9. As the loading rate becomes
9 smaller, the strain of the resistance transformation point becomes larger. This tendency may not
10 only be associated with the dilatancy characteristics of the sand but also with the pore fluid
11 migration around the cylinder.

12
13 Fig. 10 shows the time histories of the lateral resistance, the displacement of the cylinder and the
14 excess fluid pressure around the cylinder for cases SM1 and SM10. It should be noted that that
15 the base motion continued only until the end of the first half of the loading cycle in the 1 mm/s
16 loading rate case, as the period of the container shaking was 10 s. Excess pore fluid pressure of
17 the soil surrounding the cylinder of the soil was measured by the pressure transducers attached to
18 the cylinder in Fig. 4. If we look at the first cycle of the last half of the first loading cycle, in both
19 cases, the pore pressure on the side of the movement direction (the dotted line) once slightly
20 increased by the sand contraction, then it showed rapid decrease due to the sand dilation and a
21 suction force on the backside of the cylinder, while the pressure on the backside (the solid line)
22 monotonically decreased due to the suction force. As a result, the pore pressure decreased on both
23 sides when the maximum displacement of the cylinder was imposed, though the pressure on the
24 side of the direction of movement was larger than that on the other side in both cases.

25
26 Comparing the pore pressure responses between cases SM1 ($V = 1$ mm/s) and SM10 ($V = 10$
27 mm/s), it has been observed that the decrease in the pore pressure was smaller in SM1 than in
28 SM10. The displacement of the cylinder is larger in the smaller loading rate when the excess pore
29 pressure started to dissipate. This difference in the pore pressure responses may have directly
30 affected the cylinder displacement required for the lateral resistance mobilization.

31
32 Lateral resistances of the cylinder at $\gamma = \delta/D = 0.1, 0.2$ and 0.4 are plotted against cylinder
33 loading rate normalized by the soil hydraulic conductivity in the first loading in Fig. 11. The
34 lateral resistance at $\gamma = \delta/D = 0.1$ becomes remarkably larger when $V/k = 10^4$. The threshold, V/k ,
35 for the lateral resistance at $\gamma = \delta/D = 0.1$ exists between 10^3 and 10^4 for the 1-meter-diameter pile
36 (prototype) in the medium loose Toyoura sand. This threshold V/k for the lateral resistance varies

1 with δ/D , as the cylinder displacement required for the lateral resistance mobilization depends on
2 V/k .

3
4 All indications in this section support that the pore fluid migration rate, i.e., the hydraulic
5 conductivity of the soil with respect to the loading rate, is the crucial factor for mobilization of
6 the lateral resistance of a buried cylinder in liquefied soil (Takahashi et al. [12]).

7 8 **3.3. Effects of relative density on the lateral resistance**

9 Figs. 12 and 13 show the time histories of the input acceleration, deformation of the pile, lateral
10 resistance of the pile, and excess pore pressure in cases L1 and L10. It can be seen from the
11 graphs of excess pore pressures that the liquefaction occurred before cylinder loading. In Fig. 13,
12 it can be noticed that during shaking, the changes in the horizontal stress was very small but it
13 became larger after shaking has been terminated.

14
15 To evaluate the effect of the relative density on the liquefied ground, graphs of relative densities,
16 D_r , against the magnitude of horizontal stress, F_d , have been prepared as shown in Figs. 14 and 15.
17 Fig. 14 shows the relationship of the two during shaking while Fig. 15 shows after the shaking.
18 From the figures, it shows that the magnitude of horizontal stress, F_d , increases with increasing
19 value of the relative density, D_r .

20
21 When the pile is loaded, dilatancy occurs and the earth pressure becomes larger in front of the
22 pile, while at the back of the pile, the excess pore pressure decreases with the movement of the
23 pile. Furthermore, as the relative density increases, the hydraulic conductivity decreases,
24 consequently, large negative earth pressure is occurring at the back of the pile.

25
26 Figs. 16 and 17 show the relationship between the horizontal stress, F_d , and the loading rate
27 during and after shaking, respectively. It can be noticed in Fig. 16 that F_d increases with the
28 loading rate while opposite is happening in Fig. 17. During shaking, the ground behaves as a
29 viscous fluid but after shaking, when the loading rate of the cylinder increases, the magnitude of
30 horizontal stress, F_d , decreases due to the increase in the ground shear produced by the
31 occurrence of liquefaction.

32

1 **4. Conclusions**

2 The lateral resistance of the pile in liquefied soil was studied using lateral loading tests. The focus
3 of this study was to observe the deformation of the liquefied soil surrounding the pile when a
4 large relative displacement between the pile and the soil is induced. Lateral resistance of the pile
5 in the liquefying soil is directly measured by the newly developed testing apparatus. The new pile
6 loading system has the capability of applying horizontal cyclic vibrations to the pile during the
7 shaking and allowing the observation of the liquefying sand deformation. The loading rate effect
8 on the lateral resistance of the pile was also investigated. Lastly, the effect of the relative density
9 on the lateral resistance was also evaluated. The following conclusions were obtained from this
10 study:

- 11 (1) Without vibration, a large amount of soil has moved forward in front of the cylinder resulting
12 to the upheaval of the ground surface. On the other hand, when shaking was applied to the
13 container, the deformation of the soil was quite limited to the areas very close to the cylinder.
14 The difference in the soil area influenced may have directly affected the lateral resistance of
15 the cylinder for the cases of with and without shaking.
- 16 (2) Larger lateral resistance mobilization is evident as the loading rate becomes higher. The
17 lateral resistance was mobilized only after reaching a certain amount of displacement is
18 developed. As the loading rate becomes smaller, the strain of the resistance transformation
19 point becomes larger. This tendency may not only be associated with the dilatancy
20 characteristics of sand but also with the pore fluid migration around the cylinder. All
21 indications in this section support that the pore fluid migration rate, i.e. the hydraulic
22 conductivity of the soil with respect to the loading rate, is the crucial factor for mobilization
23 of the lateral resistance of a buried cylinder in liquefied soil.
- 24 (3) When the ground is in its dense condition, dilatancy occurs with the movement of the
25 cylinder. Furthermore, as the relative density increases, the hydraulic conductivity decreases,
26 consequently, large negative earth pressure is occurring at the back of the pile.

28 **References**

- 29 [1] Abdoun A, Dobry R. Seismically induced lateral spreading of two-layer sand deposit and its effect on
30 pile foundations. Proceedings of the international conference centrifuge 98, vol. 1, 1998, p. 321-8.
- 31 [2] Dobry R, Taboada V, Liu L. Centrifuge modeling of liquefaction effects during earthquakes.
32 Proceedings of the first international conference on earthquake geotechnical engineering (IS-Tokyo'95),
33 vol. 3, 1997, p. 1294-324.
- 34 [3] Hamada M, Ohtomo K, Sato H, Iwatate T. 1992, Experiment study of effects of liquefaction induced
35 ground displacement on in-ground structure. Proceedings of the fourth Japan.US workshop on earthquake
36 resistant design of lifeline facilities and countermeasures for soil liquefaction. Technical Report NCEER-
37 92-0019, vol. 1, p. 481-92.
- 38 [4] High Pressure Gas Safety Institute of Japan. Recommended practices for earthquake resistant design of
39 gas pipelines; 2000 (In Japanese).

- 1 [5] Horikoshi K, Tateishi A, Fujiwara T. Centrifuge modeling of a single pile subjected to liquefaction-
2 induced lateral spreading. *Soils and foundations, special issue on geotechnical aspects of the Jan. 17, 1995*
3 *Hyogoken.Nambu earthquake, vol. 2, 1998, p. 193-208.*
- 4 [6] Japan Society of Civil Engineers, 2000. *Earthquake resistant design codes in Japan, JSCE, Tokyo.*
- 5 [7] Metropolitan Expressway Public Corporation, 1998. *Design method for foundations subjected to*
6 *lateral spreading due to liquefaction (in Japanese).*
- 7 [8] Miyajima M, Kitaura M. Experiments on force acting of underground structures in liquefaction-
8 induced ground flow. *Proceedings of the 11th US-Japan workshop on earthquake resistant design of lifeline*
9 *facilities and countermeasures against soil liquefaction, 1994, p. 445-45.*
- 10 [9] Railway Technical Research Institute. *Seismic design for foundations, foundation design codes for*
11 *railway structures, 1997, p. 116-7 (in Japanese).*
- 12 [10] Satoh H, Ohbo N, Yoshizako K. Dynamic test on behavior of pile during lateral ground. *Proceedings*
13 *of the international conference centrifuge 98, vol. 1, 1998, p. 327-32.*
- 14 [11] Takahashi A, Takemura J, Kawaguchi Y, Kusakabe O, Kawabata N. Stability of piled pier subjected
15 to lateral flow of soils during earthquake. *Proceedings of the international conference centrifuge 98, vol. 1,*
16 *1998, p. 365-70.*
- 17 [12] Takahashi A, Kuwano J, Arai Y, Yano A. Lateral resistance of buried cylinder in yliquefied sand. In:
18 Phillips R, Guo P, Popescu R, editors. *Physical modelling in geotechnics: ICPMG'02; 2002. p. 477-82.*
- 19 [13] Takemura J, Kimura T, Suemasa N. Development of earthquake simulators at Tokyo institute of
20 technology. *Technical Report of Department of Civil Engineering Tokyo Institute of Technical, No. 40;*
21 *1989, p. 41-68.*
- 22 [14] Technical Council on Lifeline Earthquake Engineering of ASCE. 1998 Chapter 2: Experience
23 from Past Earthquakes, *Seismic Guidelines for Ports, TCLEE Monograph No. 12, ASCE.*
- 24 [15] Towhata I, Vargas-Monge W, Orense RP, Yao M. Shaking table tests on subgrade reaction of pipe
25 embedded in sandy liquefied subsoil. *Soil Dyn Earthquake Eng 1999; 18(5): 347-61.*
- 26 [16] Yasuda S, Terauchi T, Morimoto H, Erken A, Yoshida N. Post liquefaction behavior of several sands.
27 *Proceedings of 11th European conference on earthquake engineering, 1998.*

28

1 Table 1 First test condition

Case	Pore fluid material	Back pressure P_B (kPa)	Cylinder loading rate V (mm/s)	Shaking
SW1Q	Water	49	1 (Monotonic)	X
SW10Q	Water	49	10 (Monotonic)	X
SW1	Water	0	1 (Monotonic)	O
SW10	Water	0	10 (Monotonic)	O
SW100	Water	0	100 (Cyclic)	O
SM1	Methyl cel. sol.	0	1 (Cyclic)	O
SM10	Methyl cel. sol.	0	10 (Cyclic)	O
SM100	Methyl cel. sol.	0	100 (Cyclic)	O
SM10N	Methyl cel. sol.	0	10 (Cyclic)	X
SM100N	Methyl cel. sol.	0	100 (Cyclic)	X

2

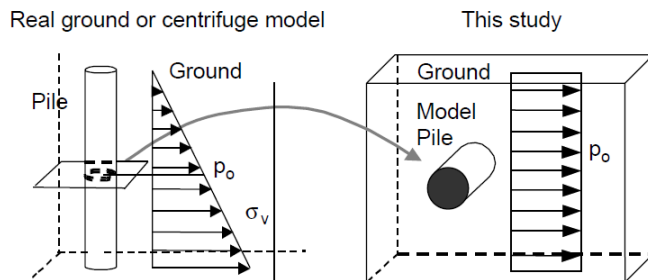
3

4 Table 2 Second test condition

Case	Relative density (%)	Cylinder loading rate V (mm/s)
L1	61	1 (Cyclic)
M1	86	1 (Cyclic)
D1	96	1 (Cyclic)
L10	64	10 (Cyclic)
M10	80	10 (Cyclic)
D10	90	10 (Cyclic)
L100	70	100 (Cyclic)
D100	93	100 (Cyclic)

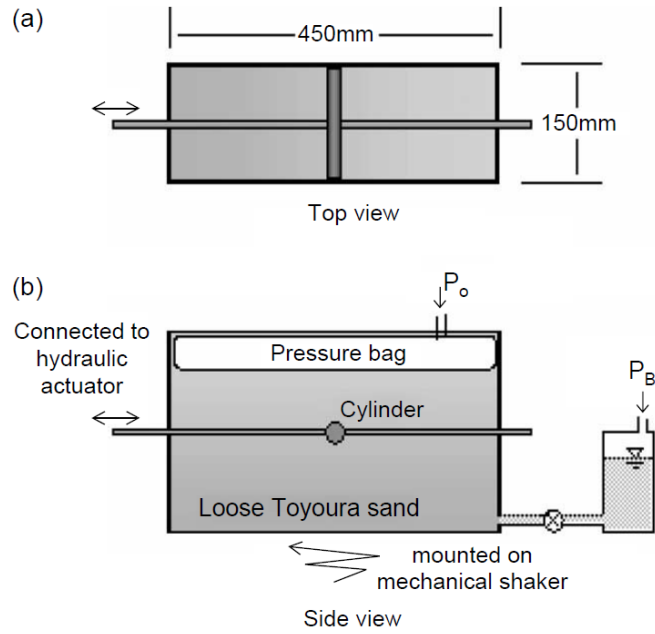
5

6

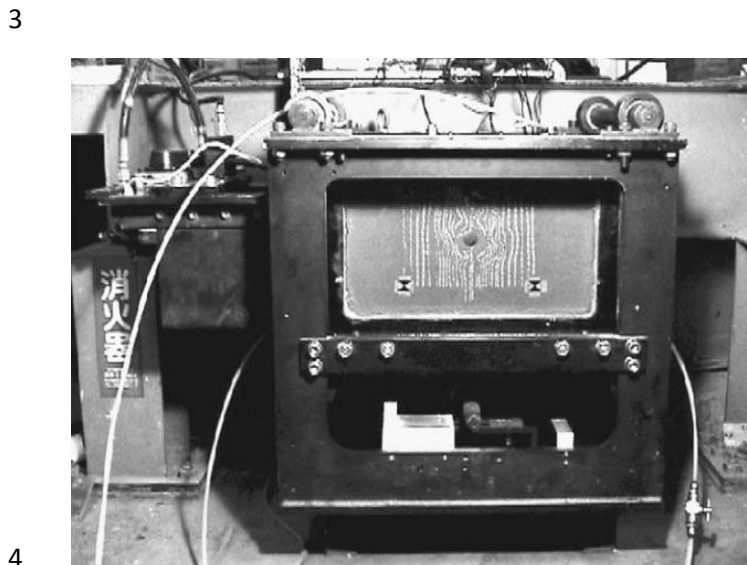


7

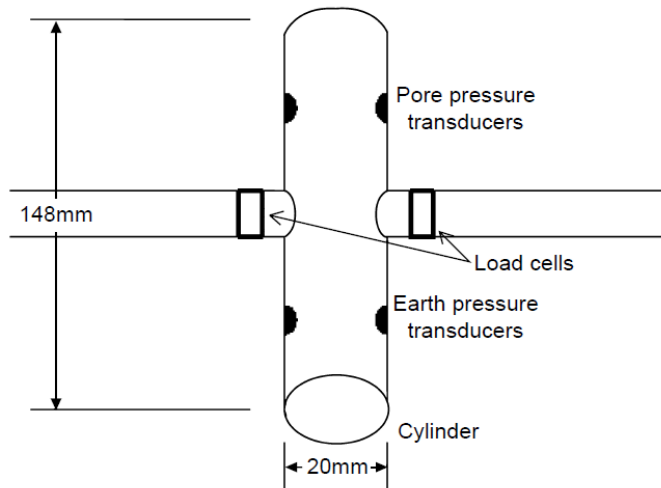
8 Fig. 1. Modeling of pile in this study.



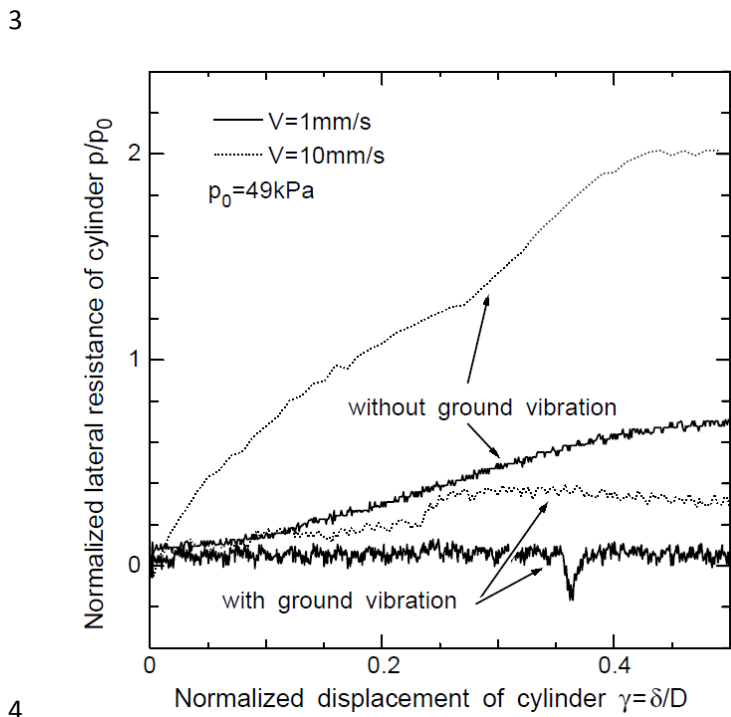
1
 2 Fig. 2. Schematic drawing of model container.



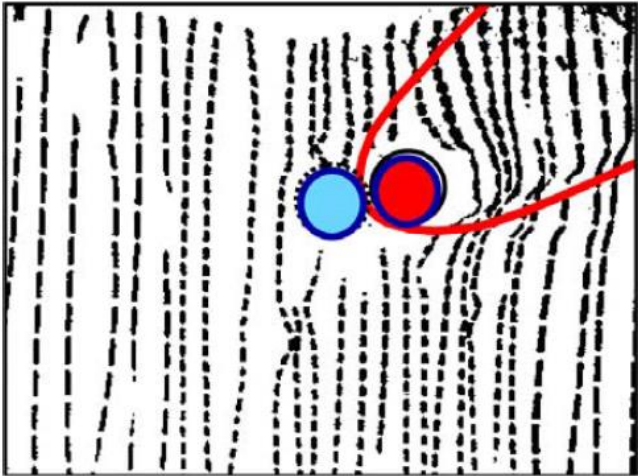
5 Fig. 3. Picture of the actual experimental setup.



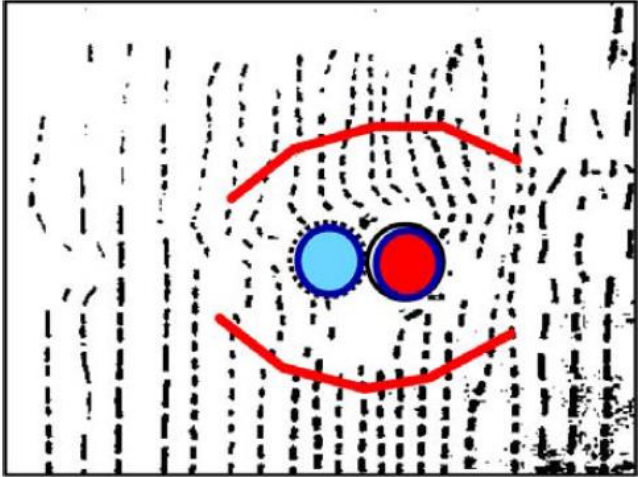
1
2 Fig. 4. Schematic drawing of the cylinder.



4
5 Fig. 5. Lateral resistance against lateral displacement of the cylinder (SW1Q, SW10Q, SW1, and SW10).

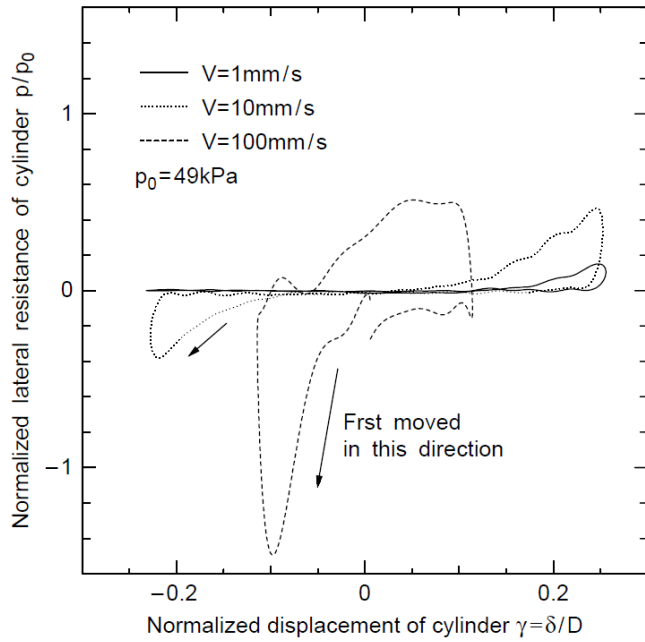


Without Ground Vibration (SW10Q)



With Ground Vibration (SW10)

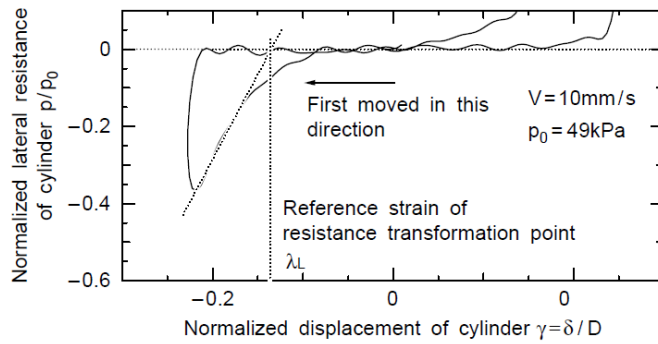
- 1
- 2 Fig. 6. Deformation of the soil surrounding the pile after loading.



1

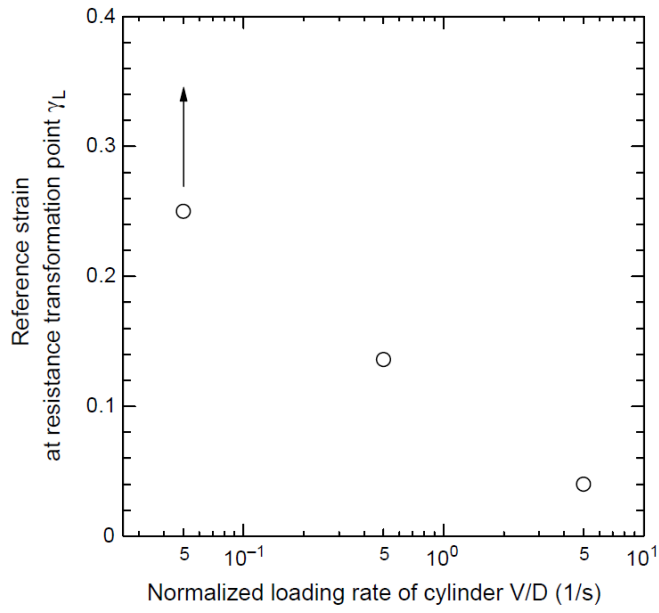
2 Fig. 7. Lateral resistance against lateral displacement of cylinder (SM1-SM100).

3



4

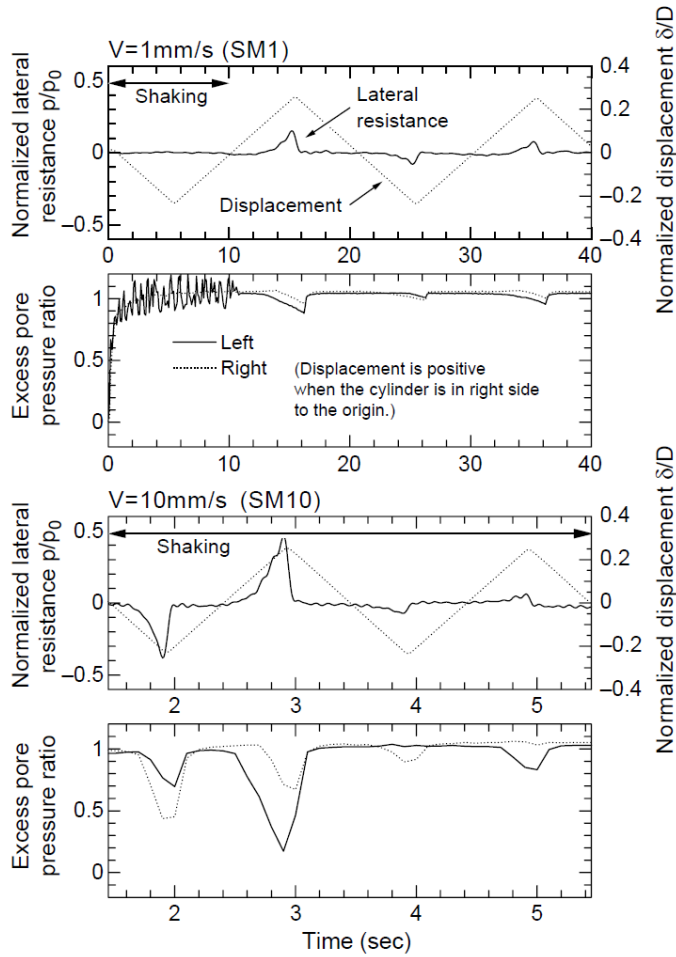
5 Fig. 8. Definition of reference strain of resistance transformation point, γ_L .



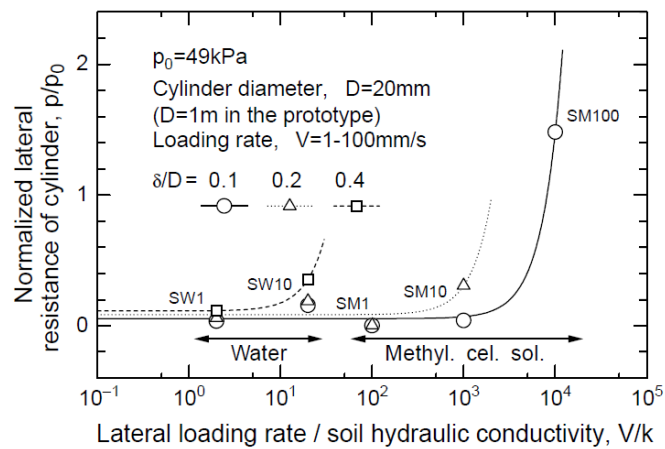
1

2 Fig. 9. Reference strain of resistance transformation point against loading rate (SM1-SM100).

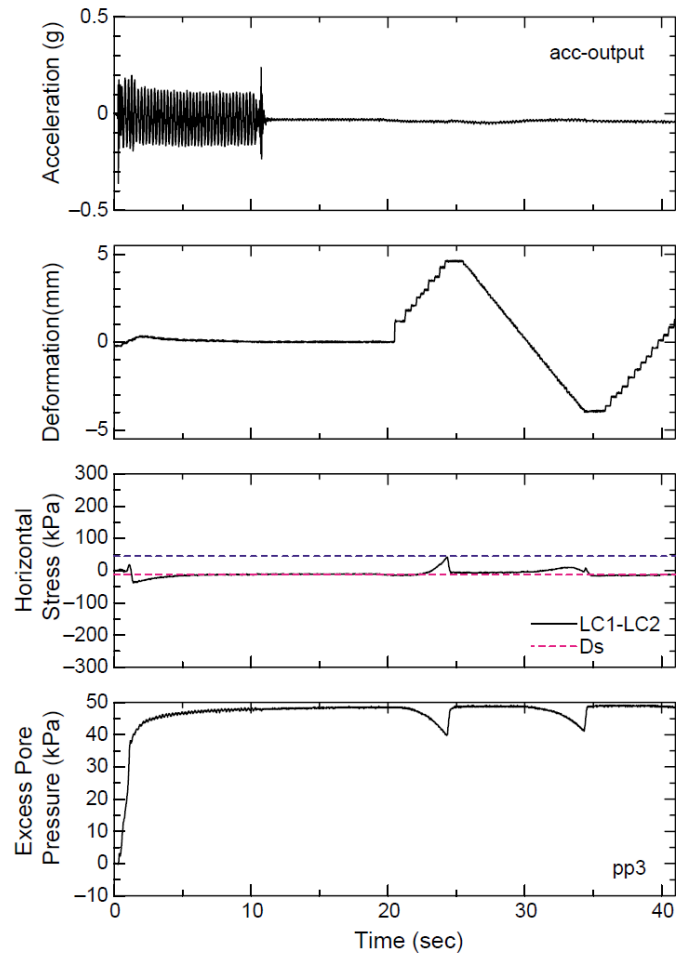
3



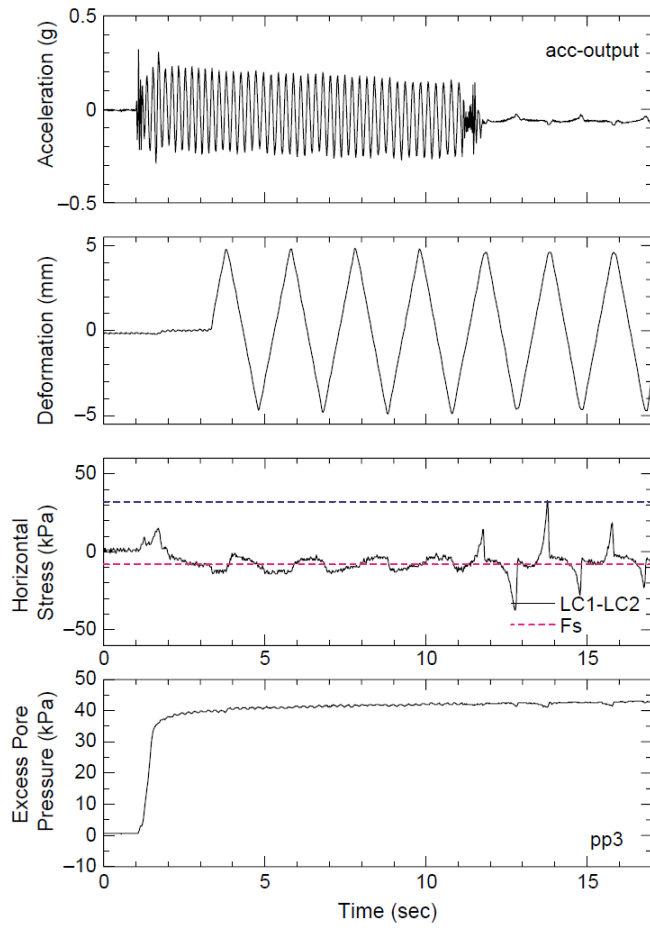
1
 2 Fig. 10. Time histories of lateral resistance and displacement of cylinder excess pore pressure around the
 3 cylinder (SM1 and SM10).



4
 5 Fig. 11. Relationship between lateral resistance of the cylinder at $\delta/D=0.1, 0.2, 0.4$ and cylinder loading
 6 rate over soil conductivity in the first loading.



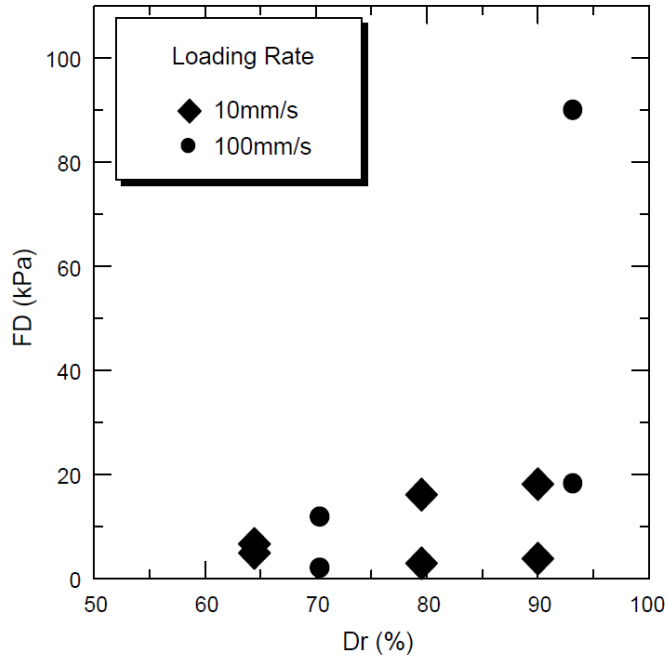
1
 2 Fig. 12. Time history of case L1.



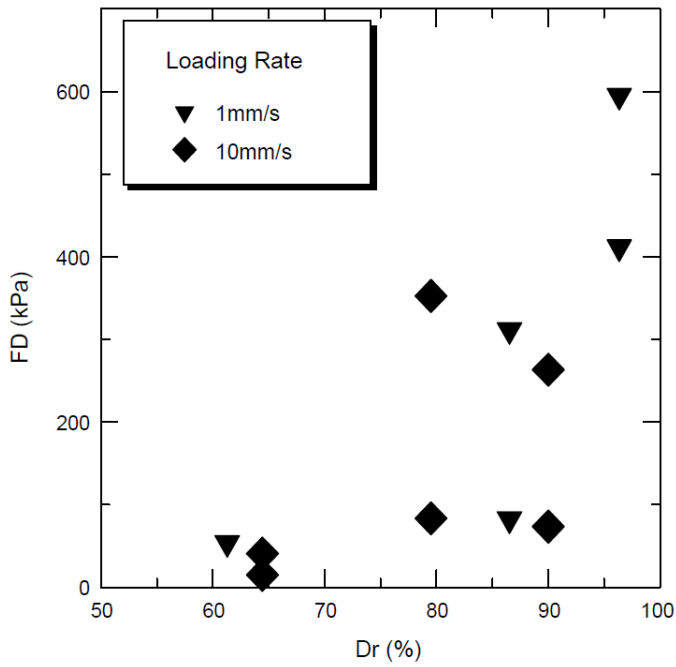
1

2 Fig. 13. Time history of case L10.

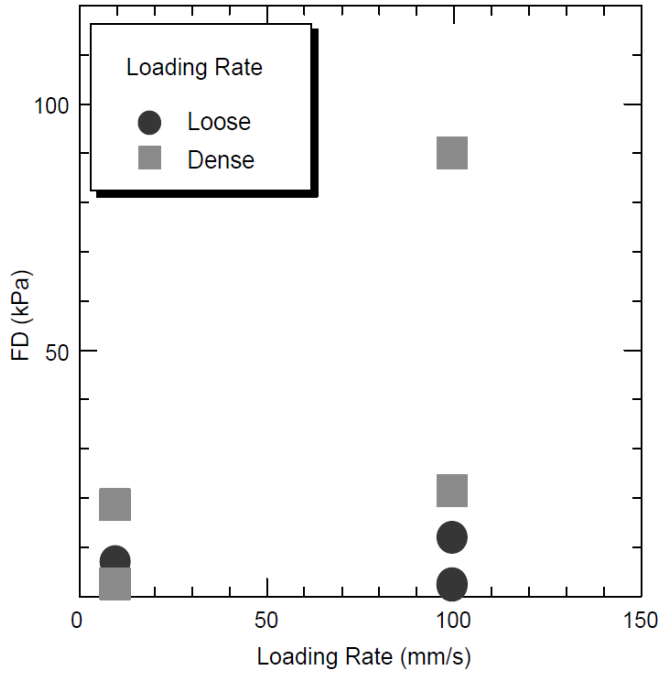
3



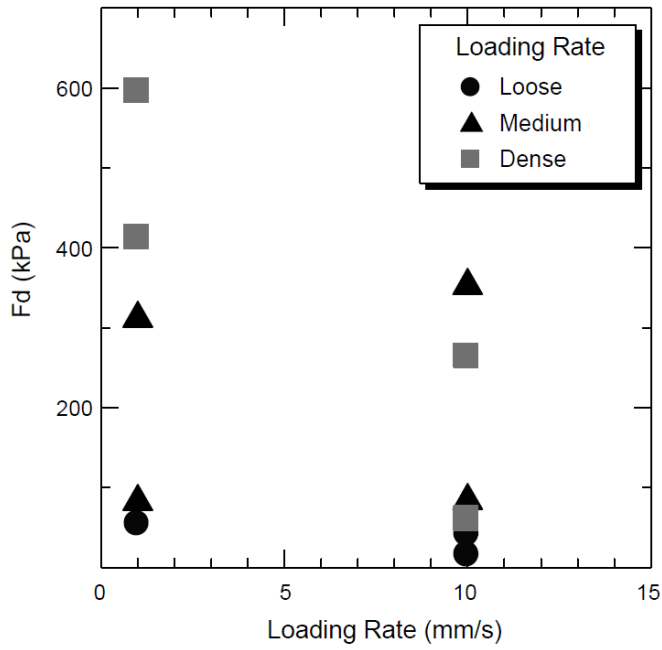
1
 2 Fig. 14. Horizontal stress against relative density during shaking.



3
 4 Fig. 15. Horizontal stress against relative density after shaking.



1
2 Fig. 16. Horizontal stress against loading rate during shaking.



3
4 Fig. 17. Horizontal stress against loading rate after shaking.
5